

# Main magnetic focus ion source: Device with high electron current density

V.P. Ovsyannikov\*

*MaMFIS Group, D-01069 Dresden, Germany*

*Joint Institute for Nuclear Research, 141980 Dubna, Russia*

A.V. Nefiodov†

*Petersburg Nuclear Physics Institute, 188300 Gatchina, St. Petersburg, Russia*

A.Yu. Boytsov, A.Yu. Ramzdorf, V.I. Stegailov, and S.I. Tyutyunnikov

*Joint Institute for Nuclear Research, 141980 Dubna, Russia*

A.A. Levin

*Ioffe Institute, 194021 St. Petersburg, Russia*

## Abstract

We discuss recent experiments performed with an upgraded version of the main magnetic focus ion source (MaMFIS) at the Joint Institute for Nuclear Research (JINR) in Dubna. The device operates in the range of electron beam energies extended up to 40 keV. The achieved electron current densities are of the order of  $10 \text{ kA cm}^{-2}$ . This assessment is consistent both with the very short ionization time and with the utmost ionization degree of the produced highly charged ions. Due to its high efficiency, the MaMFIS technology is especially promising for ionization of short-lived radionuclides. A new scheme for charge breeding is proposed.

---

\*URL: <http://mamfis.net/ovsyannikov.html>

†Corresponding author. E-mail: [anef@thd.pnpi.spb.ru](mailto:anef@thd.pnpi.spb.ru)

## I. INTRODUCTION

At present, highly charged ions are the subject of extensive research and numerous applications in atomic, nuclear, and particle physics [1–8]. High-quality beams of ions with different ionization degree for any elements and isotopes, stable and radioactive, are required. The low-energy highly charged ions are produced in ion sources both from neutral atomic targets and from externally injected low (more often singly) charged ions. In the latter case, the charge-state transformation is known as charge breeding. The most-widely-used ion sources (electron beam and electron-cyclotron resonance) operate on the basis of the successive ionization by electron impact.

A particular choice of specific characteristics of the ion beam and corresponding conditions of its production in ion sources can bring significant advantage. For example, higher ion charges  $q$  allow one to increase the precision of mass measurements in Penning traps [9]. The beams of radioactive nuclides should be bred with high efficiency much faster than they decay. For heavy isotopes with short half-lives, multiple charge stripping to  $q \gg +1$  within the confinement time of about 1 ms still poses a serious challenge as it requires a high current density  $j_e$  of the electron beam.

In this work, we describe a further development of the main magnetic focus ion source (MaMFIS), a compact room-temperature device characterized by the operating parameter  $j_e \sim 10 \text{ kA cm}^{-2}$ . Such high electron current densities are achieved in local ion traps formed in crossovers of the rippled electron beam focused by thick magnetic lens [10, 11]. This should be compared with the electron-beam ion source (EBIS) technology, which employs smooth electron flows and can attain the highest electron current density in the case of the Brillouin focusing only [12, 13]. In a crossover, the Brillouin limit is not justified and the electron current density can exceed it by orders of magnitude. We assess the magnitude of  $j_e$  indirectly by means of two quantities, namely, the ionization time and the utmost achievable charge state of the produced highly charged ions. The degree of ionization is determined from the high-energy part of the X-ray spectrum corresponding to the radiative recombination of highly charged ions with beam electrons. We suggest a novel scheme for charge breeding, which is most promising to use in the rare-isotope beam facilities, which require low-intensity bunches of highly charged ions to be produced at a high repetition rate.

## II. EXPERIMENTAL SETUP

The experimental setup realized at JINR includes a modified MaMFIS and an X-ray detector for spectroscopy studies of highly charged ions (see Fig. 1). The Dubna MaMFIS operates with electron beams characterized by the current  $I_e$  of up to 50 mA (in direct current mode) and the extended electron energy

$E_e$  of up to 40 keV. The focusing system utilizes permanent magnets. The typical basic vacuum is on the level of about  $10^{-9}$  mbar. The drift tube consists of three sections with a total length of 30 mm.

In order to estimate the charge state distributions of the trapped ions, the characteristic emission was recorded in the energy range of radiative recombination. A typical X-ray spectrum exhibits radiation peaks originated from ionization of different electron shells. Since energy of the recombination lines is given by the sum of electron beam energy  $E_e$  and ionization energy, the charge states of recombined ions can be unambiguously determined.

Besides testing the ionization ability by X-ray spectroscopy (in the running mode indicated in Fig. 2(a)), we controlled for the behavior of ions in the MAMFIS by EBIS technology (in the running modes indicated in Figs. 2(b) and 2(c)). This can be achieved due to the fact that for a certain length-to-diameter ratio of the drift tube, the extracting potential penetrates into the drift tube and opens local ion traps (see Fig. 2(c)). Accordingly, three types of potential distributions of the electric field in the direction of the electron beam ( $z$  axis) were employed in our experimental tests of the device. An equal potential applied to all the parts of the electron-optical system (the anode and the two sections of the drift tube) provides the necessary condition for axial confinement and subsequent ionization of highly charged ions in local traps. The radial confinement is due to the space charge of electron beam and the magnetic field. In Fig. 2(a), the depth of potential well is determined by depth of the local ion traps formed by crossovers of rippled electron beam ( $\Delta U = \Delta U_1$ ). In Fig. 2(b), the anode A and the outer section  $S_2$  of the drift tube are positively biased with respect to the central section  $S_1$  to form the axial potential barriers ( $\Delta U > \Delta U_1$ ). The time dependence of the potential distributions in accordance with the EBIS technology [12] allows one to extract ions pre-produced in discrete local ion traps. In this case, the confinement time  $\tau$  is determined as the time delay between sequential switches of the potential distributions depicted in Figs. 2(b) and 2(c).

### III. IONIZATION ABILITY

In Fig. 3, the X-ray emission spectra due to radiative recombination of highly charged ions of the cathode materials (Ir and Ce) and injected Xe gas with beam electrons are presented. The Dubna MaMFIS is able to ionize all atomic species up to  $M$ -shell of Ir and  $L$ -shells of Ce and Xe. The feature of the experiments consists in consideration of a steady-state plasma. It means that all direct and reverse processes, such as ionization, charge exchange, radiative recombination, heating and cooling are in a dynamic equilibrium. The electron current density is a key factor affecting the ionization rates and times. A high magnitude of  $j_e$  is the necessary condition for achievement of the highest charge states of trapped ions. The maximum ionization degrees of highly charged ions ( $\text{Ir}^{67+}$ ,  $\text{Ce}^{56+}$ , and  $\text{Xe}^{52+}$ ) produced in the Dubna MaMFIS are

consistent with the electron current density  $j_e$  of the order of  $10 \text{ kA cm}^{-2}$ . This estimate is confirmed by the computer simulations of ionization processes in the ion trap under experimental conditions [14].

#### IV. CONTROL OVER BEHAVIOR OF IONS IN LOCAL ION TRAPS

The electron beam current density in local ion traps can also be estimated by studying the dependence of the radiative recombination spectra on the ionization time. For this purpose the running mode with variable potential distribution as indicated in Figs. 2(b) and 2(c) was implemented.

The time dependence of the X-ray spectrum of radiative recombination for a mixture of cathode materials (Ir and Ce) and injected Ar gas is presented in Fig. 4(a). The spectra exhibit growth of both the ionization degree and number of photon counts with increasing confinement time. This is in agreement with the theoretical predictions. An important conclusion can be drawn from the radiation spectrum for the confinement time  $\tau$  of 1 ms. This time is sufficient for complete ionization of the  $M$ -shell of cerium and  $K$ -shell of argon. The result indicates that the electron current density of about  $10 \text{ kA cm}^{-2}$  is achieved experimentally. The computer simulations performed for experimental conditions also confirm the conclusion (see Fig. 4(b)).

The control over behavior of highly charged ions in local ion traps by changing the potential distribution in the drift tube allows one to employ the MaMFIS technology for charge breeding of low charged ions.

#### V. MAMFIS-BASED CHARGE BREEDER

In Fig. 5, a new scheme for charge breeding is presented with an indication of the electron and ion trajectories and the corresponding electric potential distributions. The process of charge breeding consists of four technological stages. During the first stage, low charge state ions are injected from an external ion source through the extractor electrode E and the electron collector C (see Fig. 5(a)). During the second stage, the low charged ions are captured into the longitudinal ion trap. The trap is closed, when a positive bias is superimposed on the outer section  $S_2$  of the drift tube (see Fig. 5(b)). These are the same procedures as in the standard EBIS-based charge breeder, since they are carried out in a smooth electron beam of a constant radius. In the third stage, the smooth electron flow is transformed into a rippled beam by varying the potential of the focusing (Wehnelt) electrode W (see Fig. 5(c)). The ions are now confined in local ion traps and stripped of bound electrons up to the desired high charge states. This combination of the EBIS and MaMFIS technologies can make it possible to achieve an extremely high electron current density. During the fourth stage, the highly charged ions are extracted from the breeder either in the axial (see Fig. 5(d)) or

radial direction [10].

The question concerning the efficiency of our proposed scheme for charge state breeding requires further experimental investigation. However, there is already experience of using a small warm electron beam ion trap as a charge breeder, in which the capture and breeding efficiencies of about 0.02% for  $\text{K}^{17+}$  were measured [15]. Leaving aside the problem of ion optics for the injection and extraction stages, we note that the breeding efficiency significantly depends on the particular charge states to be produced. This is mainly because the degree of the space charge compensation declines at higher ion charges  $q$ . In contrast to the EBIS, the MaMFIS technology, owing to its extremely high electron current density, reduces significantly the confinement time required for an efficient ionization of bound electrons. This result is of particular importance both for heavy elements and for very short-lived radionuclides. In particular, fast ionization of inner-shell electrons can allow one to eliminate the internal conversion decay channels, so that the half-lives of nuclides can be increased by orders of magnitude. Accordingly, it seems feasible to expand the amount of short-lived radioactive species available for precision mass measurements in Penning traps.

## VI. CONCLUSIONS

Our experiments with the upgraded MaMFIS version in Dubna confirm the high ionization ability of this technology for production of highly charged ions. The ion source has been tested at electron beam energies of up to  $E_e = 22.5$  keV. The ionization degree  $q = +67$  of iridium ions was achieved. The argon atoms are ionized completely within about 1 ms. These results are consistent with the electron current density of the order of  $10 \text{ kA cm}^{-2}$ . The possibilities for control over the ion behavior in local ion traps have also been investigated. This opens a way to design ion sources with extremely short times of charge breeding.

### Acknowledgements

The authors are grateful to E.D. Donets, E.E. Donets, D.E. Donets, V.V. Karpukhin, A.N. Nukin, D.O. Ponkin, D.N. Rassadov, V.V. Salnikov, and A.A. Smirnov for their support of the experimental studies.

- 
- [1] F. Wenander, *J. Instr.* **5**, C10004 (2010).
  - [2] D. Rodríguez, K. Blaum, W. Nörtershäuser, M. Ahammed, A. Algora, G. Audi, J. Äystö, D. Beck, M. Bender, J. Billowes, et al., *Eur. Phys. J. Special Topics* **183**, 1 (2010).
  - [3] M. C. Simon, J. C. Bale, U. Chowdhury, B. Eberhardt, S. Ettenauer, A. T. Gallant, F. Jang, A. Lennarz, M. Luichtl, T. Ma, et al., *Rev. Sci. Instr.* **83**, 02A912 (2012).

- [4] A. Thorn, E. Ritter, F. Ullmann, W. Pilz, L. Bischoff, and G. Zschornack, *Rev. Sci. Instr.* **83**, 02A511 (2012).
- [5] A. Y. Boytsov, D. E. Donets, E. D. Donets, E. E. Donets, K. Katagiri, K. Noda, D. O. Ponkin, A. Y. Ramzdorf, V. V. Salnikov, and V. B. Shutov, *Rev. Sci. Instr.* **86**, 083308 (2015).
- [6] A. Lapierre, G. Bollen, D. Crisp, S. W. Krause, L. E. Linhardt, K. Lund, S. Nash, R. Rencsok, R. Ringle, S. Schwarz, et al., *Phys. Rev. Accel. Beams* **21**, 053401 (2018).
- [7] M. G. Kozlov, M. S. Safronova, J. R. Crespo López-Urrutia, and P. O. Schmidt, *Rev. Mod. Phys.* **90**, 045005 (2018).
- [8] A. Lapierre, *Rev. Sci. Instr.* **90**, 103312 (2019).
- [9] K. Blaum, S. Eliseev, and S. Sturm, *Quantum Sci. Technol.* **6**, 014002 (2020).
- [10] V. P. Ovsyannikov and A. V. Nefiodov, *Nucl. Instr. Meth. B* **367**, 1 (2016).
- [11] V. P. Ovsyannikov and A. V. Nefiodov, *Nucl. Instr. Meth. B* **370**, 32 (2016).
- [12] E. D. Donets, USSR Inventor's Certificate No. 248860, 16 March (1967), *Bull. OIPOTZ* 24 (1969) 65.
- [13] E. D. Donets, *Rev. Sci. Instr.* **69**, 614 (1998).
- [14] I. V. Kalagin, D. Küchler, V. P. Ovsyannikov, and G. Zschornack, *Plasma Sour. Sci. Technol.* **7**, 441 (1998).
- [15] G. Vorobjev, A. Sokolov, A. Thorn, F. Herfurth, O. Kester, W. Quint, T. Stöhlker, and G. Zschornack, *Rev. Sci. Instr.* **83**, 053302 (2012).

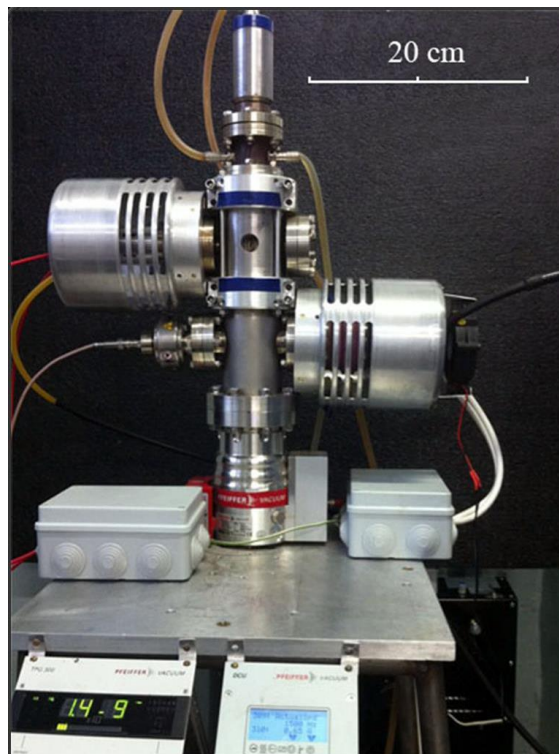
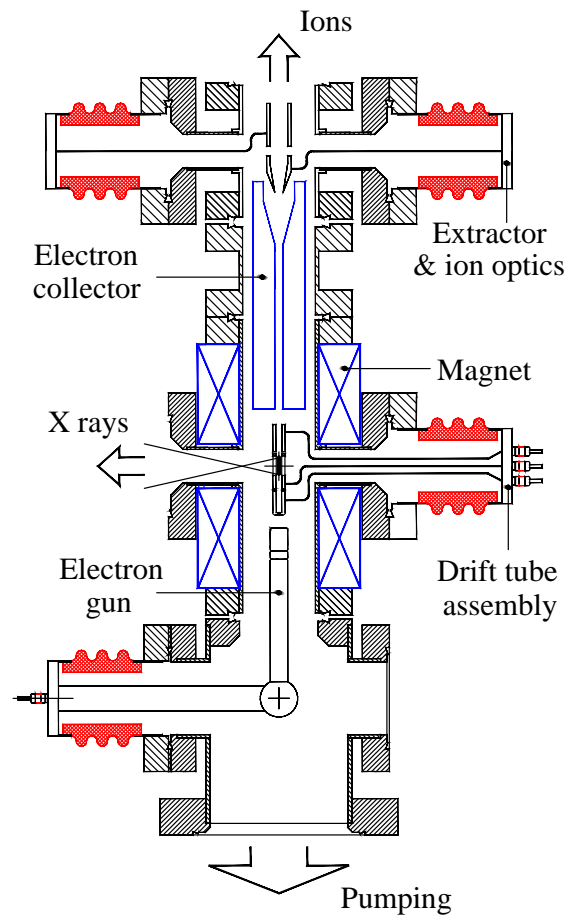


FIG. 1: Dubna MaMFIS: principle scheme and general view (photo) of the construction.

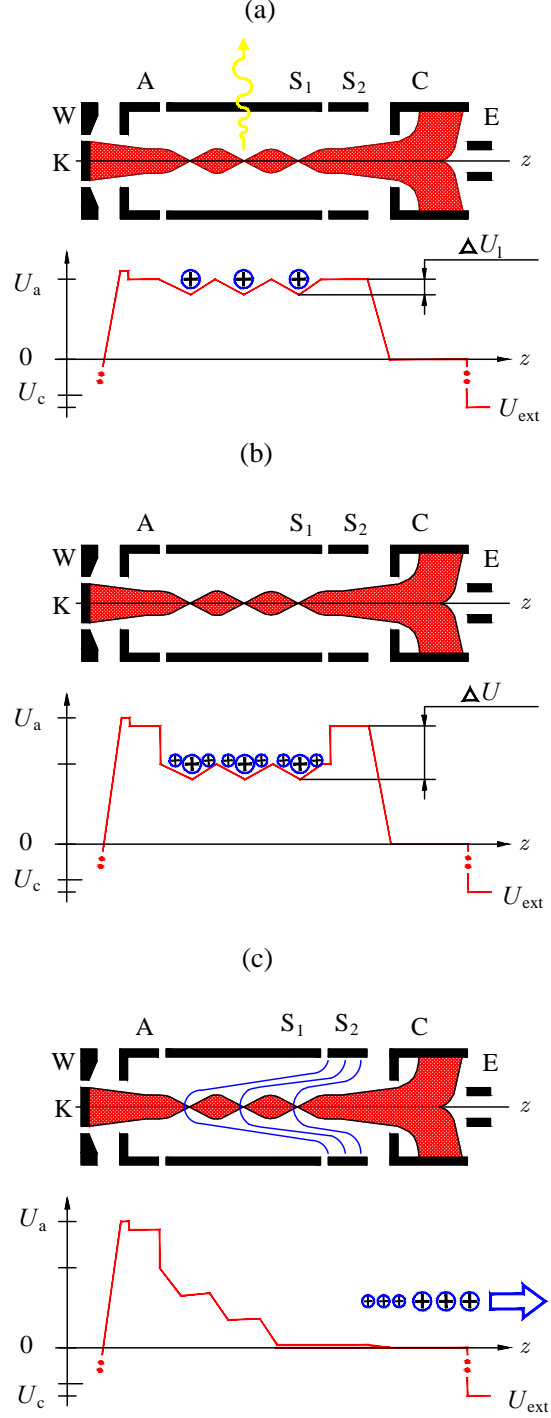


FIG. 2: Schemes of electric potential distributions for different running modes. (a) MaMFIS running mode. (b) and (c) Combined MaMFIS/EBIS running mode. The notations are the following: cathode K, focusing (Wehnelt) electrode W, anode A integrated with the first section of the drift tube, separate sections ( $S_1$  and  $S_2$ ) of the drift tube, electron collector C, extractor E, cathode potential  $U_c$ , anode potential  $U_a$ , extractor potential  $U_{\text{ext}}$ , depth  $\Delta U_1$  of a local trap, and depth  $\Delta U$  of the common trap ( $\Delta U \geq \Delta U_1$ ). The encircled plus signs denote highly charged ions. The local ion traps appear in the crossovers of rippled electron beam, which are formed in focuses of thick magnetic lens.



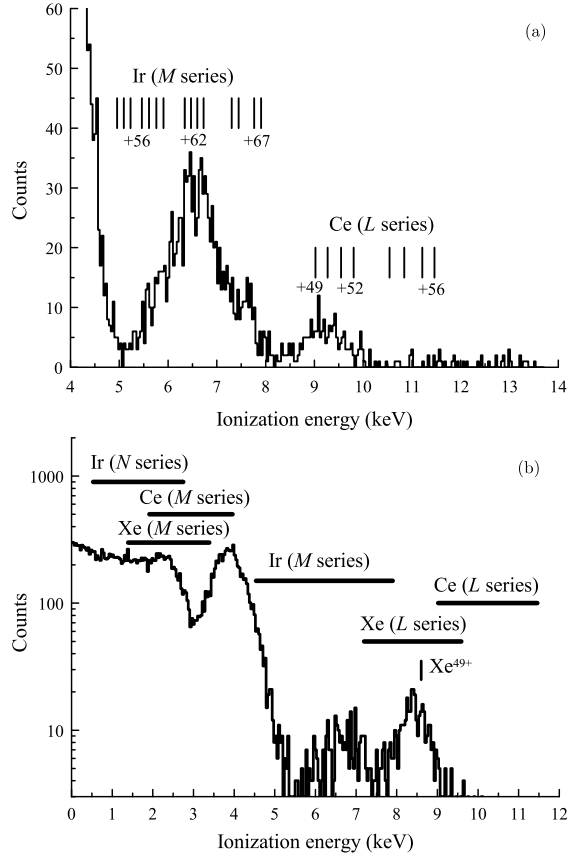


FIG. 3: Radiative recombination spectrum for cathode materials (a) and xenon (b). The ionization energy is defined as the difference between the energy of emitted photons and the electron beam energy  $E_e = 22.5$  keV. Vacuum during the measurements was in the range from  $5 \times 10^{-9}$  to  $2 \times 10^{-8}$  mbar.

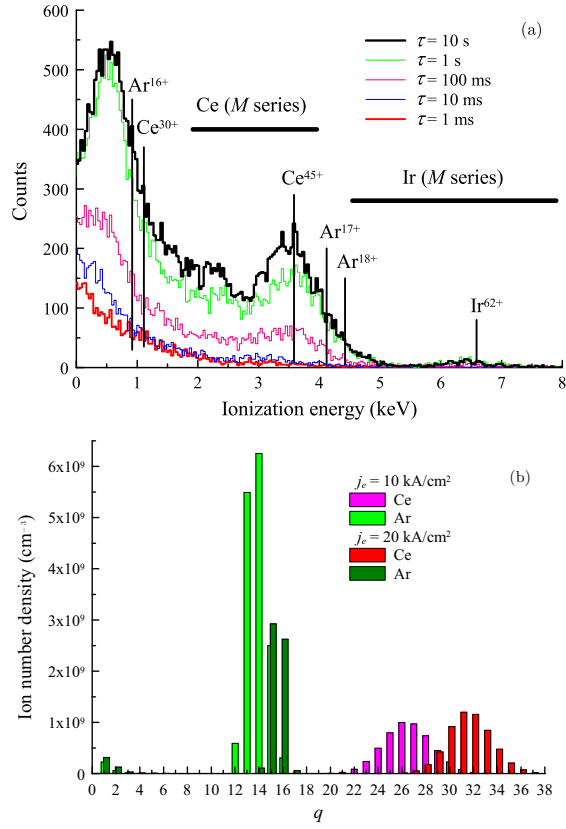


FIG. 4: (a) Evolution of the spectrum of cathode materials and argon ions as dependent on the confinement time  $\tau$ . (b) Computer simulations for charge-state distributions of Ar and Ce ions ( $\tau = 1$  ms and  $j_e = 10$  and  $20$  kA cm<sup>-2</sup>).

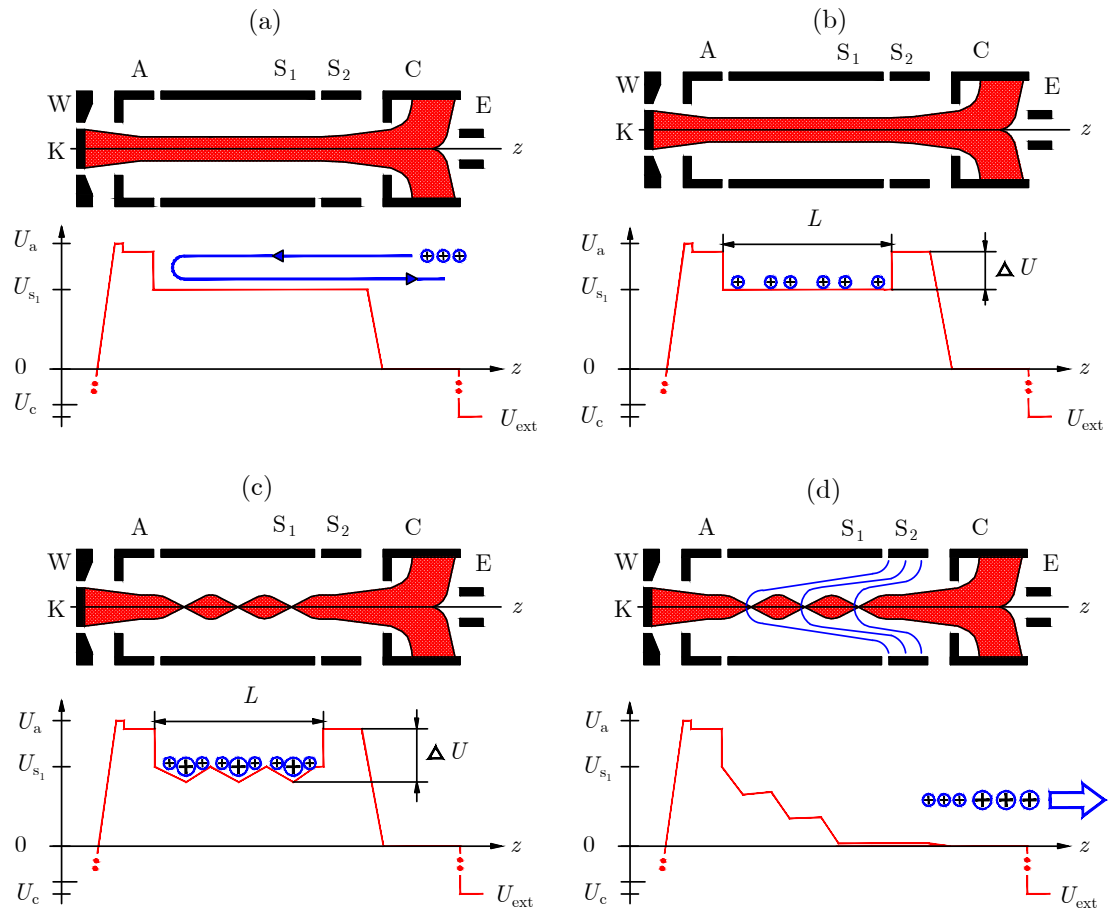


FIG. 5: MaMFIS as a charge breeder. Symbol  $L$  denotes length of common trap,  $U_{s_1}$  is electric potential at section  $S_1$  of the drift tube.